

## Vertical seismoelectric profiling in a borehole penetrating glaciofluvial sediments

J. C. Dupuis<sup>1</sup> and K. E. Butler<sup>1</sup>

Received 22 March 2006; revised 12 June 2006; accepted 29 June 2006; published 16 August 2006.

[1] Seismoelectric signals have been measured as a function of depth in a borehole penetrating glaciofluvial sands, silts, and glacial till using a broadband surface seismic source, and a downhole electrode array. Transient electric field pulses, with amplitudes of 1 to 4  $\mu\text{V}/\text{m}$  accompanied the arrival of seismic P-waves at the electrodes but no simultaneous interfacial signals were observed above the noise floor of approximately 0.2  $\mu\text{V}/\text{m}$ . The co-seismic effect was strongest in a sand and gravel layer where its amplitude is consistent with the predictions of a simplified theoretical model. Normalization of the amplitude logs by measurements of seismic particle velocity and electrical conductivity enhanced their sensitivity to changes in lithology and porosity. The results of this experiment suggest that co-seismic seismoelectric effects show potential as a porosity/permeability logging tool in the borehole environment. **Citation:** Dupuis, J. C., and K. E. Butler (2006), Vertical seismoelectric profiling in a borehole penetrating glaciofluvial sediments, *Geophys. Res. Lett.*, 33, L16301, doi:10.1029/2006GL026385.

### 1. Introduction

[2] Seismoelectric signals of electrokinetic origin are produced when charge in the electrical double layer at solid-liquid interfaces in porous or fractured media is disturbed by seismically induced fluid flow. They are of interest in both hydrogeology and hydrocarbon reservoir exploration/characterization for the information they may be able to provide regarding pore fluid type, porosity and fluid flow permeability.

[3] While our conceptual understanding of the seismoelectric effect has improved in recent years, the theory that predicts the existence of these signals has outstripped our ability to measure and interpret them in the field. In this work, we present high resolution field measurements of seismoelectric effects generated in porous sediments using a surface to borehole geometry that was expected to be sensitive to both co-seismic effects generated in the immediate vicinity of the receiver and interfacial effects emanating from nearby geological contacts. Similar borehole experiments have been reported by Hunt and Worthington [2000] and by Mikhailov *et al.* [2000] but they utilized different seismic sources (a downhole hammer and Stoneley waves respectively) and focused on the characterization of fractured rock.

### 2. Description of the Experiment

#### 2.1. Test Site Characteristics

[4] Monitoring borehole, UNB1-03, located in Fredericton, New Brunswick, Canada, was installed as part of a previous hydrogeophysical study [Nadeau, 2005] and lined with slotted PVC casing below a bentonite seal at 12 m depth in order to allow for electrical logging. The 40 m meter borehole penetrated through fluvial sands, a thick glaciolacustrine clay/silt aquitard, silty sand and gravel from the flanks of the esker-like Fredericton aquifer, and glacial till interbedded with outwash sand and gravel as shown in Figure 1. It was inaccessible below 35 m depth because of sediment infiltration. The data for this experiment were acquired during the summer and fall of 2005 during which time the water level in the borehole remained at 9.2 m depth.

#### 2.2. Seismoelectric Measurements

[5] Electrodes were constructed from 10 AWG stranded copper wire wrapped around 10 cm segments of 2.5 cm diameter PVC pipe. They were connected to a multi-paired cable and the connections waterproofed with marine epoxy. The resulting array included four electrodes centered 2.2 m apart on the end of a 40 m cable. The measurements reported here were made by pairing the electrodes so as to give three dipoles each 2.2 m in length as shown in Figure 1. The signals from the dipoles were buffered using custom-built differential preamplifiers which provided a gain of 30 and then recorded by a 24-bit seismograph (Geometrics Geode) using a sample interval of 0.125 ms. To avoid cross-talk, the seismoelectric data were acquired separately from the seismic and all other data.

[6] In order to bypass the surficial sands and deliver seismic energy directly to the water saturated aquitard we drilled a second borehole, 1.5 m away from UNB1-03, to a depth of 9.2 m. The hole was lined with PVC casing, and a pole constructed from multiple 1.5 m sections of 2.54 cm PVC conduit was inserted until it reached the end cap. The pole was centered in the borehole by rubber spacers (constructed from hockey pucks). A small sledgehammer was used to tap on a protective wooden cap at the top of the pole, and an accelerometer mounted on the cap was used to trigger the seismograph.

[7] The seismoelectric data were acquired at night when the powerline harmonic noise was weakest and most stable. The amplitude of the harmonic noise at this time of the day was about half of that measured during the afternoon, ranging from 500  $\mu\text{V}/\text{m}$  in the most resistive sediments near the bottom of the hole to 100  $\mu\text{V}/\text{m}$  in the more conductive clay/silt unit.

[8] The electrode array was lowered to the bottom of the borehole and raised in increments of 55 cm - a spacing

<sup>1</sup>Department of Geology, University of New Brunswick, Fredericton, New Brunswick, Canada.

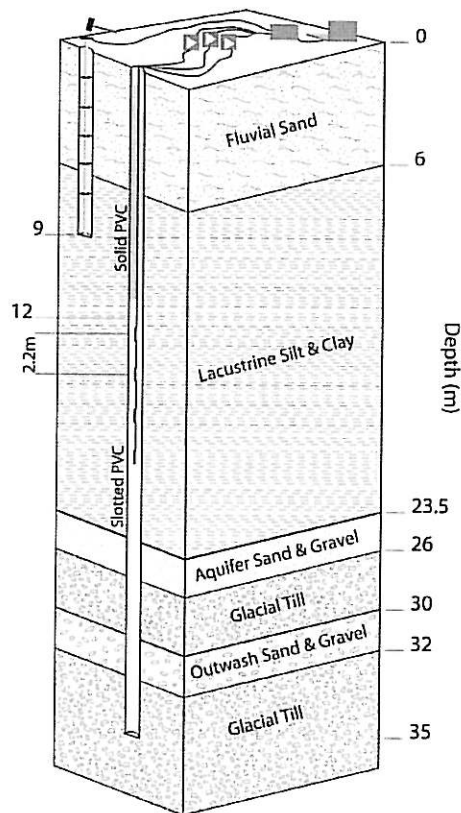


**Figure 1.** Geological log and experimental setup for vertical seismoelectric profiling at borehole UNB1-03.

chosen to facilitate stacking of the signal from dipoles at common depths. Twenty shots were acquired at every depth, thereby providing sufficient data for a fold of 60 traces per depth taking into account the redundancy offered by the three dipoles.

[9] After acquiring a full set of seismoelectric data at 55 cm spacing, the measurements were repeated at depths intermediate between those sampled the first time. The two data sets together sampled the borehole at 27.5 cm intervals and demonstrated good repeatability.

### 2.3. Other Borehole Logs

[10] A borehole resistivity log was acquired at 10 cm intervals using a 'normal' resistivity probe connected to a resistivity meter (ABEM SAS 300) at surface. The probe was constructed using 5.08 cm ABS pipe and tinned copper wire. The short and long separations between the current electrode and potential electrodes were 20 cm and 1 m respectively.

[11] A borehole geophone, containing two vertical elements with natural frequencies of 14 and 28 Hz, was also constructed and used to measure the amplitude of the seismic P-wave arrival as a function of depth. Measurements were made at 50 cm intervals and five shots were recorded at every depth. We also had access to gamma ray, P-wave velocity and S-wave velocity logs and to measurements of water content/porosity based on sediment

sampling, all of which had been documented by Nadeau [2005].

## 3. Processing of the Data

### 3.1. Seismoelectric

[12] Given the weakness of the seismoelectric signals relative to the ambient electrical noise, the raw field records did not show any signs of seismoelectric signal. The raw data were filtered with a 100–500 Hz Butterworth bandpass filter and then processed with the harmonic noise subtraction algorithm of Butler and Russell [2003]. The processed shot records were inspected and those exhibiting high residual noise were killed in order to avoid contamination of the stacks.

[13] Upon inspection of the shot records, we discovered that they suffered from triggering errors which degraded the quality of our original common depth stacks. Statics corrections were applied prior to stacking in order to compensate for this problem. The signal to noise improvement by harmonic subtraction and by stacking was between 40 and 60 dB.

### 3.2. Seismic

[14] The raw geophone records were bandpass filtered in the same way as the seismoelectric data. Noisy traces were killed and the remaining traces were stacked according to depth. Geophone voltages were converted to particle veloc-

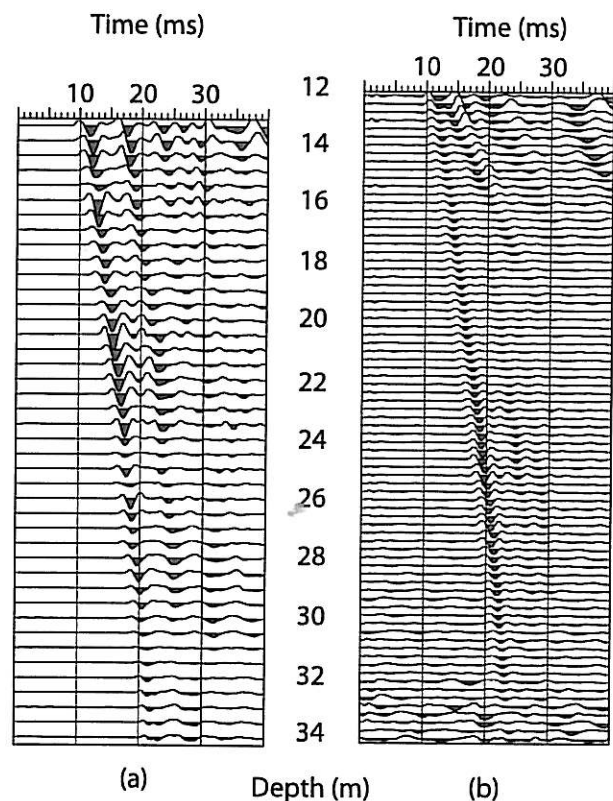


**Figure 2.** (a) Seismic and (b) seismoelectric arrivals as a function of depth in borehole UNB1-03. The traces in each compilation are plotted at their true relative amplitudes.

**Table 1.** Value of the Variables Used to Compute the Expected Seismoelectric Response in the Sands of the Aquifer

Material property	Symbol	Value	Units
Electrical conductivity	$\sigma$	10	mS/m
Zeta potential	$\zeta$	-50	mV
Electrical permittivity	$\epsilon_f$	80 $\epsilon_0$	F/m
Fluid viscosity	$\eta$	1	mPa s
Porosity	$\beta$	35	%
Tortuosity	$\tau$	1.92	-
Poroelastic constant	$Q$	$1.31 \times 10^9$	N/m <sup>2</sup>
Poroelastic constant	$R$	$7.10 \times 10^8$	N/m <sup>2</sup>
P-wave velocity	$v$	1650	m/s
Characteristic velocity	$v_c$	1719	m/s
Particle velocity	$\dot{u}$	$7.5 \times 10^{-6}$	m/s
Angular frequency	$\omega$	$2\pi \times (335)$	rad/s
Bulk modulus (solid) <sup>a</sup>	$K_s$	$37.9 \times 10^9$	N/m <sup>2</sup>
Bulk modulus (fluid) <sup>a</sup>	$K_f$	$2.25 \times 10^9$	N/m <sup>2</sup>
Bulk modulus (dry frame) <sup>a</sup>	$K_{fr}$	$2.20 \times 10^8$	N/m <sup>2</sup>

<sup>a</sup>Values required to compute  $Q$  and  $R$  from *Biot and Willis* [1957].

ities using the transduction constant for the appropriate geophone element.

#### 4. Results

[15] Figure 2 shows vertical profiles of the stacked seismic and seismoelectric records, both plotted with true relative amplitudes. The co-seismic seismoelectric signal can be followed along the entire depth of the borehole although the signal to noise ratio degrades at depth, victim of weaker seismic signals and greater noise levels caused by the higher resistivity of the glacial till and the outwash sand and gravel. Amplitude variations are apparent as we progress down the borehole and cross into different types of sediments.

[16] It is also evident that the dominant frequency of the co-seismic seismoelectric data is higher than that of the seismic. The dominant frequency estimated from the first arrival pulse width is  $\approx 380$  Hz for the co-seismic seismoelectric and  $\approx 290$  Hz for the seismic. This increase is consistent with the linear frequency dependence in equation (1) presented below. Also, since we are measuring a potential difference as opposed to a true electric field measurement, the electrode spacing can become significant in terms of the seismic wavelength and contribute to the shape of the spectrum. The effect of spatial filtering will be investigated in future work.

[17] A second type of seismoelectric response, emanating from interfaces in porous media and appearing simultaneously on widely separated antennas, has also been reported, and predicted by theory. We had anticipated that such signals might be generated by P-waves arriving at the clay/sand or sand/till contacts but no such events are evident above the noise level of approximately  $0.2 \mu\text{V/m}$  in our processed data.

#### 5. Validation of a Theoretical Model

[18] Co-seismic seismoelectric signals are generated in the immediate vicinity of the receiving dipole. Thus, for dipoles contained within a single layer it seems reasonable that the signals may be approximately modelled as if they were in unbounded homogeneous media. Plane wave solutions for fully coupled seismic and electromagnetic waves

in homogeneous, poroelastic media have been derived by *Pride and Haartsen* [1996]. *Garambois and Dietrich* [2001] reported that co-seismic seismoelectric signal strengths measured at surface were consistent with predictions based on a low frequency form of that theory. In this case, we compare our borehole measurements to an alternative model, developed by *Neev and Yeatts* [1989] which has received less attention in the literature. The model is simpler and less general than that of *Pride and Haartsen* [1996] in that it ignores electromagnetic effects and any frequency dependence of physical properties. Plane wave solutions for seismoelectric effects expected to accompany seismic P-waves were instead derived by treating the problem as quasi-static and modifying Biot's poroelastic equations of motion to account for electric forces that would arise due to electrokinetic coupling. We anticipate that this approximation may be adequate for order of magnitude estimates at seismic frequencies.

[19] The transfer function, given by *Neev and Yeatts* [1989] in non-dimensional form, relating co-seismic seismoelectric effects to P-wave particle motions in the low frequency limit may be expanded as follows [*Butler*, 1996]:

$$E \approx \frac{-j\omega\epsilon_f\zeta(Q+R)}{\sigma\tau^2\eta v_c v} \dot{u}. \quad (1)$$

[20] Here,  $E$  is the electrical field,  $\dot{u}$  is the particle velocity,  $\omega$  is the angular frequency,  $\epsilon_f$  is the fluid permittivity,  $\zeta$  is the zeta potential,  $Q$  and  $R$  are poroelastic constants defined by *Biot and Willis* [1957],  $\sigma$  is the conductivity,  $\tau$  is the tortuosity,  $\eta$  is the fluid viscosity,  $v_c$  and  $v$  are phase velocities.

[21] Using equation (1) it is possible to compute an expected electrical field for the sand and gravel aquifer. Our in-situ measurements, found in Table 1, provide values for all the variables except for the  $\zeta$  potential and the tortuosity  $\tau$ .

[22] The  $\zeta$  potential for most water-saturated geological sediments, according to *Ishido and Mizutani* [1981] and *Morgan et al.* [1989], ranges between  $-10$  mV and  $-100$  mV; we choose  $-50$  mV as an intermediate value. The porosity measurements in the sand and gravel can be converted into tortuosity if we assume that the grains are spherical and we use the relation proposed by *Berryman* [1980],  $\tau = (1 + 1/\beta)/2$ , where  $\beta$  is porosity. With these estimates for  $\zeta$  and  $\tau$  and the rest of the values found in Table 1, the expected electrical field in the sand and gravel aquifer is  $10.7 \mu\text{V/m}$ . This is within a factor of three of the measured amplitude of  $3.8 \mu\text{V/m}$ . Thus, given the uncertainty in the values of  $\tau$  and  $\zeta$ , the quasi-static theory of *Neev and Yeatts* [1989] seems to provide a reasonable explanation for the origins of the co-seismic seismoelectric signals observed in this case.

#### 6. Discussion

[23] In order to better see the effects of sediment type on the strength of the co-seismic seismoelectric signal, the amplitudes of the first pulse were measured and plotted versus depth in Figure 3 alongside logs of seismic amplitude, electrical conductivity, natural gamma radiation, and

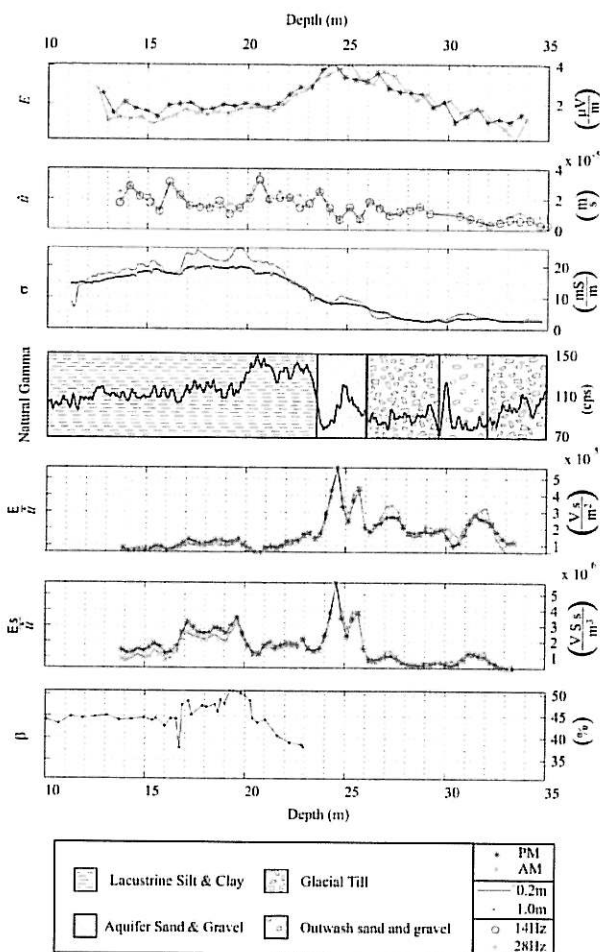


**Figure 3.** Comparison of the seismoelectric log  $E$  to logs of particle velocity  $\dot{u}$ , conductivity  $\sigma$ , geology, natural gamma, and porosity  $\beta$ . Normalized logs, compensated for variations in  $\dot{u}$  and  $\sigma$ , are also shown.

geology. It is clear that the seismoelectric response is strongest in aquifer sand and gravel unit and weakest in the clay/silt unit, but efforts to understand the source of these variations are complicated by the dependence (as postulated in equation (1)) on seismic particle velocity and electrical conductivity. Two normalized seismoelectric logs were calculated in order to address that ambiguity.

[24] We first normalized to account for the variations in particle velocity. The normalized log  $E/\dot{u}$  shown in Figure 3 is better at differentiating between the aquifer and its surroundings. Its response is low through the clay/silt aquitard and increases in the aquifer before decreasing again in the glacial till. There is also evidence of an inverse relationship between  $E/\dot{u}$  and natural gamma ray emissions that are normally indicative of clay content. The abrupt increases in the gamma ray log at 20.5, 25, and 30 m for example are all correlated with drops in  $E/\dot{u}$ .

[25] The response of the  $\dot{u}$ -normalized log is clearly weakest in the clay/silt aquitard. This can be explained to some extent, however, by the relatively high electrical conductivity of the clay/silt unit, which would naturally

lead to more shunting of any electrokinetic effects generated in it. In order to remove this ambiguity, we can compensate the seismoelectric log for both particle velocity and conductivity. This dual normalization ( $E\sigma/\dot{u}$ ), as shown in Figure 3, increases the response in the clay/silt while decreasing it in the till. It also yields an anomalously strong response from a 3 m thick portion of the clay/silt that correlates exactly with the zone of elevated porosity that exists between 17 m and 20 m in the final panel of Figure 3.

[26] These normalized seismoelectric logs demonstrate that the strong seismoelectric response observed in the aquifer sands cannot be attributed to variations in particle velocity or electrical conductivity alone. Other factors are responsible for the noted increase in the sand and gravel aquifer. Laboratory measurements on the sediment samples retrieved from UNB1-03 may allow us to measure the  $\zeta$  potential and determine its role in the seismoelectric highs observed but porosity and pore space tortuosity (which are in turn related to fluid flow permeability) and elastic constants must play an important role in the seismoelectric amplitudes observed.

## 7. Conclusions

[27] Co-seismic seismoelectric effects were successfully acquired in a borehole which penetrates glaciofluvial sediments using a high resolution surface seismic source. It was shown that these signals vary with sediment type and that normalization can increase the sensitivity of the seismoelectric log to parameters which may be of interest in determining fluid flow permeability.

[28] Although seismoelectric signals from interfacial effects at this site were too weak to be measured, surface to borehole or vertical seismoelectric profiling experiments hold great potential for helping to determine the types of interface that are most amenable to detection. They also offer a systematic method to validate theoretical models that exist for seismoelectric effects in layered media. In this case, we have shown that the low frequency limit of a simple quasi-static model for co-seismic seismoelectric effects in homogeneous media was able to reproduce signal strengths we measured in a sand layer to within a factor of three.

[29] The field experiment and analyses presented here are of general interest in light of ongoing efforts to determine how seismoelectric effects may be applied to assess pore fluid type, porosity and fluid flow permeability in aquifers or reservoirs. They also suggest that co-seismic seismoelectric effects, normally considered to be noise in surface seismoelectric experiments, have potential to be used as a porosity/permeability logging tool in the borehole environment.

[30] **Acknowledgment.** Funding for this project was provided by the Natural Sciences and Engineering Research Council of Canada in the form of a Discovery Grant to K. E. Butler and a Postgraduate Scholarship to J. C. Dupuis.

## References

- Berryman, J. G. (1980), Long wavelength propagation in composite elastic media, I. spherical inclusions, *J. Acoust. Soc. Am.*, 68, 1809–1819.
- Biot, M. A., and D. G. Willis (1957), The elastic coefficients of the theory of consolidation, *J. Appl. Mech.*, 24, 594–601.



- Butler, K. E. (1996), Seismoelectric effects of electrokinetic origin, Ph.D. thesis, Univ. of B. C., Vancouver, B. C., Canada.
- Butler, K. E., and R. D. Russell (2003), Cancellation of multiple harmonic noise series in geophysical records, *Geophysics*, 68, 1083–1090.
- Garambois, S., and M. Dietrich (2001), Seismoelectric wave conversions in porous media: Field measurements and transfer function analysis, *Geophysics*, 66(5), 1417–1430.
- Hunt, C. W., and M. H. Worthington (2000), Borehole electrokinetic responses in fracture dominated hydraulically conductive zones, *Geophys. Res. Lett.*, 27, 1315–1318.
- Ishido, T., and H. Mizutani (1981), Experimental and theoretical basis for electrokinetic phenomena in rock-water systems and its application to geophysics, *J. Geophys. Res.*, 86, 1763–1775.
- Mikhailov, O. V., J. Queen, and M. N. Toksöz (2000), Using borehole electroseismic measurements to detect and characterize fractured (permeable) zones, *Geophysics*, 65, 1098–1112.
- Morgan, F. D., E. R. Williams, and T. R. Madden (1989), Streaming potential properties of westerly granite with applications, *J. Geophys. Res.*, 94, 12,449–12,461.
- Nadeau, J. C. (2005), Geophysical imaging of a river valley aquifer, Master's thesis, Univ. of N. B., Fredericton, N. B., Canada.
- Neev, J., and F. R. Yeatts (1989), Electrokinetic effects in fluid-saturated poroelastic media, *Phys. Rev. B*, 40, 9135–9141.
- Pride, S., and M. W. Haartsen (1996), Electrostatic wave properties, *J. Acoust. Soc. Am.*, 100, 1301–1315.

---

K. E. Butler and J. C. Dupuis, Department of Geology, University of New Brunswick, P.O. Box 4400, Fredericton, NB, Canada E3B 5A3. (kbutler@unb.ca; c.dupuis@unb.ca)